826. Seismic analysis of the condensate storage tank in a nuclear power plant

Wei-Ting Lin[1], Meng-Hsiu Hsieh[2], Yuan-Chieh Wu[3], Chin-Cheng Huang[4]
[1, 2, 3, 4]Institute of Nuclear Energy Research, Atomic Energy Council
Executive Yuan, Taoyuan 325, Taiwan, R. O. C.
[1]Department of Civil Engineering, National Ilan University, Ilan 260, Taiwan, R. O. C.
E-mail: [1]*wtlin@iner.gov.tw*, [2]*marshall94216@iner.gov.tw*, [3]*ycwu@iner.gov.tw*, [4]*cchuang@iner.gov.tw*

(Received 12 July 2012; accepted 4 September 2012)

Abstract. Following the nuclear power plant accident in Fukushima Japan, seismic capacity evaluation has become a crucial issue in combination building safety. Condensate storage tanks are designed to supplies water to the condensate transfer pumps, the control rod drive hydraulic system pumps, and the condenser makeup. A separate connection to the condensate storage tank is used to supply water for the high pressure coolant injection system, reactor core isolation cooling system, and core spray system pumps. A condensate storage tank is defined as a seismic class I structure, playing the important role of providing flow to the operational system and the required static head for the suction of the condensate transfer pumps and the normal supply pump. According to the latest nuclear safety requirements, soil structure interaction must be considered in all seismic analyses. This study aims to rebuild the computer model of condensate storage tanks in Taiwan using the SAP 2000 program in conjunction with the lumped mass stick model and to evaluate the soil structure interaction by employing the SASSI 2000 program. The differences between the results with the soil structure interaction and spring model are compared via natural frequency and response spectrum curves. This computer model enables engineers to rapidly evaluate the safety margin of condensate storage tank following the occurrence of earthquakes or tsunamis.

Keywords: soil structure interaction, response spectrum analysis, spectral acceleration.

Introduction

Taiwan is situated on the circum-Pacific seismic belt that has created a large number of devastating earthquakes over past decades. Those devastating earthquakes such as Kobe, Tang-Shan, and Chi-Chi have resulted in severe structural damage to buildings. The recent earthquake and subsequent tsunami in Tohoku caused critical damage to key structures of the Fukushima nuclear power plant and leakage resulted in considerable damage to the property and health of nearby residents as well as to the economy as a whole [1, 2]. Three of four nuclear power plants in Taiwan are located near Taipei, the capital city of Taiwan, and the safety of these power plants is a matter of grave concern to authorities and the general public. The evaluation of seismic capacity of combination buildings at a nuclear power plant is a key aspect in evaluating the safety of a plant.

The Condensate and Feedwater system, including the condensate storage tank (CST), provides for the collection of exhaust steam from the main turbine and the reactor feed pumps into the main condenser. The system also maintains the required capacity and flow of condensate for the high pressure coolant injection (HPCI) and reactor core isolation cooling (RCIC) systems and will maintain a proper level in the condenser hotwell. In addition, the CST also provides flow to the other systems as required and provides the required static head for the suction of the condensate transfer pumps and the normal supply pump. Each generator is provided with supply lines to ensure that both units are supplied. Thus, CSTs are considered seismic category I structures and play the important role for the nuclear power plant safety.

The effect of soil structure interaction (SSI) has generally been neglected in the dynamic analysis of civil engineering structures. However, it is important for the dynamic analysis of

NPPs. The SSI effect should be considered as one of the dynamic characteristics of NPP buildings if the effect is too large to ignore [3]. Neglecting SSI is acceptable for light structures in relatively stiff soil such as low rise buildings and simple rigid retaining walls. However, the effect of SSI becomes more prominent for heavy structures resting on relatively soft soils such as nuclear power plants, high-rise buildings and elevated-highways on soft soil [4]. Damage sustained in recent earthquakes has also highlighted how the seismic behavior of a structure is highly influenced not only by the response of the superstructure, but also by the response of the foundation and the ground [5]. In addition, with standard review plan 3.7.2 promulgated by the latest United States Nuclear Regulatory Commission (USNRC) [6], the effect of SSI in seismic system analysis should be considered conscientiously. Over the last few decades, there has been a dramatic increase in the use of dynamic response analysis of SSI in nuclear power plants [7-10], and the effect of SSI has also been considered in bridges and buildings [11, 12]. Nonetheless, there has been relatively little research in this area.

The operating period of the nuclear power plants in Taiwan is approaching the designed lifespan of 40 years. Although close to the end of their service, they are still functioning well. Nonetheless, an approach must be devised to evaluate the safety of NPPs in the event of a loss of power before their expiry or extended service date. According to the latest USNRC standards, seismic capacity evaluation including SSI is a significant aspect of NPP safety. This study aims to rebuild the computer model of CST in Taiwan using the SAP 2000 program by the lumped mass stick model, and to further evaluate SSI using SASSI 2000. The SSI model was generated and compared the differences between the results with the SASSI and spring model, and was compared via the natural frequency and response spectrum curves.

Lumped Mass Stick Model

This study rebuilds the computer model of the CST by employing the SAP 2000 program in conjunction with the lumped mass stick model. Natural frequency analysis and floor response spectrum curves for the spring model were generated and a comparison of the differences in natural frequency between the original and rebuilt model was performed.

To compare the natural frequency between the original and rebuilt model of the CST, seismic input parameters should be in accordance with the original calculations performed in 1986 [13]. Input data should include the design ground time history, damping, soil parameters, and the properties of the lumped mass stick model. The properties of the lumped mass stick model of CST for horizontal and vertical model are listed in Tables 1 and 2, respectively.

Table 1. Lumped mass properties of CST for horizontal model

Mass point	Weight (kips)	I (ft^4)	Shear area (ft^2)	Material type
1	30.9	-	-	Steel
2	436.5	1023.93	3.274	Steel
3	621.4	1023.93	3.274	Steel
4	622.8	1023.93	3.274	Steel
5	684.9	1023.93	3.274	Steel
6	750.0	1280.32	4.093	Steel
7	751.8	1598.45	5.108	Steel
8	-	1927.11	6.153	Concrete
9	4092.0	1116000	3720	Concrete
10	-	1116000	3720	Concrete

Figure 1 shows a horizontal synthetic earthquake ground acceleration time history, in which the input motion is the East-West component of the recorded motion in the free-field at the grade level [14]. The maximum horizontal ground acceleration is 0.157 g, and the time history

has a duration of 44 s. In addition, the floor response spectrum, generated from the ground acceleration time history, adequately envelops the design response spectrum, as specified in the regulatory guide 1.60 in the frequency range of 0.5 to 100 Hz.

Table 2. Lumped mass properties of CST for vertical model

Mass point	Weight (kips)	I (ft^4)	Shear area (ft^2)	Material type
1	30.9	-	-	Steel
2	7.64	1023.93	3.274	Steel
3	8.82	1023.93	3.274	Steel
4	10.25	1023.93	3.274	Steel
5	11.03	1023.93	3.274	Steel
6	14.88	1280.32	4.093	Steel
7	16.72	1598.45	5.108	Steel
8	7890.60	1927.11	6.153	Steel

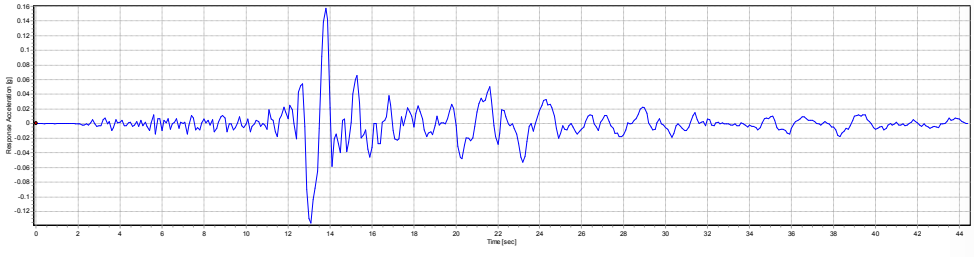

Fig. 1. Horizontal synthetic curve of acceleration time history

The damping values are in accordance with regulatory guide 1.61. The reinforced concrete structure and welded structure of the CST have values of 0.07 % and 0.04 %, respectively. Soil structure interaction is represented mathematically by the equivalent massless foundation spring, in accordance with the original calculations.

Lumped mass stick models with springs were developed for the CST, and a horizontal model and a vertical model are shown in Figs. 2 and 3, respectively. Discrete mass points are provided at major floor elevations and at locations of structural discontinuity. The properties of the stick model beam elements, including the locations of the centroid, centers of rigidity, and centers of mass, as well as the equivalent sectional areas and moments of inertia, were computed using specific finite element sections representing the principal floor elevations of the structures. Based on previous calculations, the lumped masses comprise dead loads, live loads, and equipment. In addition, the elastic springs K_x (1.33×105 k/ft) and K_θ (1.282×108 k-ft/rad) of the horizontal model and K_y (2.74×105 k/ft) of the vertical model represent the interconnectors between the structures and soil.

Final Element Model for SSI

This study generated a computer model of a CST using SASSI 2000 with the SSI model. The analysis model for the structure is used a multi-lumped mass system with the rigid basemat slab. In SASSI, the structural model is generated as a lumped mass stick model which consists of a steel tank and a reinforced concrete basemat. In addition, the spectral acceleration curves generated from the SASSI models are compared and discussed. The response spectrum curves of the CST model with the SSI effect and spring model are also discussed.

Three-dimensional seismic SSI analysis of nuclear related structures is often performed in the frequency domain using programs such as SASSI. For the soil model, a SASSI site model

was constructed from the average strain-compatible soil properties obtained from free-field SHAKE deconvolution analysis using the horizontal components of the recorded motion of the earthquake event [14]. The properties of the soil obtained from a geophysical field survey and the strain-dependent shear modulus and damping ratios obtained from dynamic triaxial and resonant column test results were used in the SHAKE analysis as listen in Table 3. The CST was modeled using a 3D lump mass stick model, and a natural frequency analysis model was generated from the same model as illustrated in Fig 4. Input motion was also determined using the recorded motion in Lotung [14].

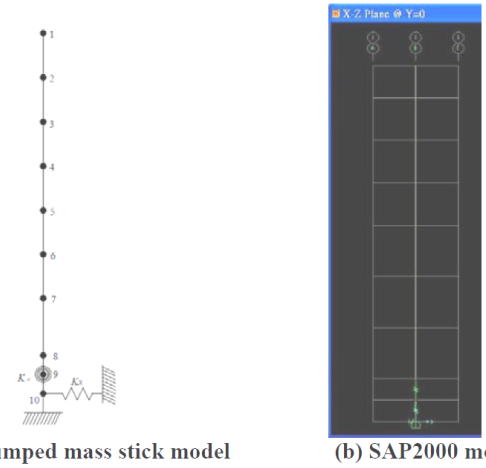

(a) Lumped mass stick model (b) SAP2000 model

Fig. 2. Lumped mass stick model of CST horizontal model

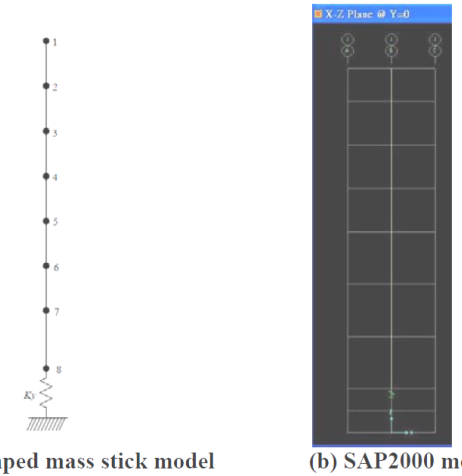

(a) Lumped mass stick model (b) SAP2000 model

Fig. 3. Lumped mass stick model of CST vertical model

For the soil model, a SASSI site model was constructed from the average strain-compatible soil properties obtained from free-field SHAKE deconvolution analysis using the horizontal components of the recorded motion of the earthquake event [14]. The soil properties obtained from the geophysical field survey along with the strain-dependent shear modulus and damping ratios obtained from dynamic triaxial and resonant column test results were used in the SHAKE analysis. For the structural model, the CST was modeled using a 3D lump mass stick model,

whose natural frequency analysis model was generated in the same manner. In addition, the input motion also used the recorded motion in Lotung [14].

Table 3. SASSI soil profile model

Elevation (ft)	Layer no.	Depth (ft)	*Vs* (ft/s)	*Vp* (ft/s)	γ (kcf)
0	1	4	253	1290	0.134
-4	2	4	253	1290	0.134
-8	3	4	253	1290	0.134
-12	4	3	253	1290	0.134
-15	5	4.6	253	1290	0.134
-19.6	6	5	253	1290	0.134
-24.6	7	5.5	301	1534	0.123
-30	8	6	301	1534	0.123
-36	9	5	301	1534	0.123
-41	10	5	391	1994	0.128
-46	11	5	391	1994	0.128
-51	12	5	391	1994	0.128
-56	13	9	391	1994	0.128
-65	14	9	391	1994	0.128
-74	15	8	391	1994	0.128
-82	16	8	391	1994	0.128
-90	17	8	391	1994	0.128
-98	18	8	391	1994	0.128
-106	19	8	529	2697	0.124
-114	-	-	536	2733	0.117

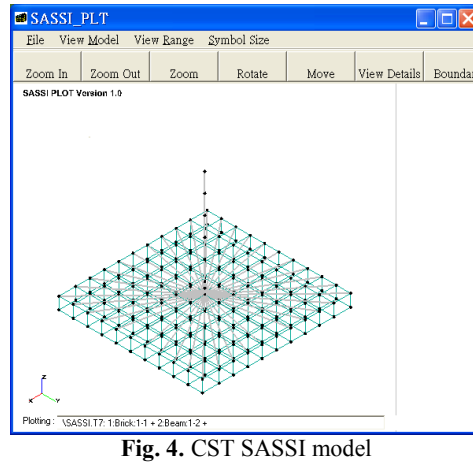

Fig. 4. CST SASSI model

This study selected a CST model to simulate the soil profile for the SASSI program. The model is the structural finite element model, which includes the lumped mass superstructure and basemat shown in Fig. 4. The basemat was modeled using 100 solid elements connected to the underlying soil at 242 nodes. The basemat model was discretized at an elevation of 0 ft and the CST was connected to the bottom of the basemat at an elevation of 0 ft by a series of rigid links.

Results and Discussion

A comparison of natural frequencies between the rebuild and previous results for the horizontal and vertical model are summarized in Table 4. The natural frequencies generated by

the new horizontal and vertical model are close to those generated by the previous model from modes 1 and 1 to 2, respectively (below ±5 %). In horizontal and vertical direction, the major mode is observed at frequency of 3.18 Hz and 5.29 Hz giving a participation mass ratio of 79.41 % and 99.99 %, respectively. More mass participation in vertical direction is attributed to the presence of rigid in the structure. A comparison of the 1st and 2nd mode shape in the new and previous model for the horizontal and vertical model is illustrated in Figs. 5 to 6, respectively. The natural frequency mode shapes generated by the new horizontal and vertical model coincide with those generated by the previous model.

Table 3. Comparison of the natural frequency for the horizontal and vertical model

Model No.	Horizontal model				Vertical model			
	Natural frequency (Hz)			Model participating mass ratio (%)	Natural frequency (Hz)			Model participating mass ratio (%)
	Rerun	Previous	Variation		Rerun	Previous	Variation	
1	3.18	3.11	2.20 %	79.41	5.29	5.29	0 %	99.99
2	7.84	6.72	14.29 %	18.40	83.92	85.20	1.53 %	0.01
3	24.14	14.65	39.31 %	1.50	-	-	-	-

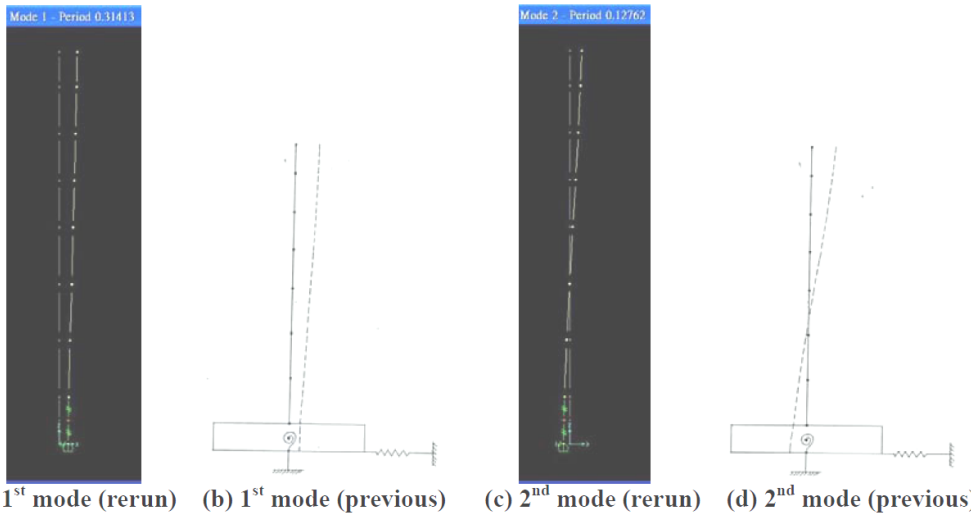

(a) 1st mode (rerun) (b) 1st mode (previous) (c) 2nd mode (rerun) (d) 2nd mode (previous)

Fig. 5. Comparison of the natural frequency mode shape in the rerun and previous horizontal models

The results of the floor response spectrum curves generated by the dynamic analysis of the rebuilt model for fixed-end are presented in Fig. 7. The response spectra consider the input dispersion through a 15 % extension in the frequency range, in accordance with regulatory guide 1.122. In this model, nodes 8, 9, and 10 were generated to simulate the basemat of CST using a rigid link, resulting in similar floor response spectrum curves among those nodes. The zero period accelerations (ZPA) in nodes 1 to 7 and 9 are 0.4026 g, 0.3870 g, 0.3622 g, 0.335 g, 0.3017 g, 0.2646 g, 0.2288 g and 0.1874 g, respectively, which are consistent with the results generated from the previous model.

Prediction of the seismic response of a CST according to the SSI effects is generally subject to a number of uncertainties. These include the definition of free-field ground motion, variability in soil and structural properties, idealization of the soil-structure system, and differences in SSI analysis techniques. Considerable uncertainty arises from the idealization of the soil-structure system. In this study, the results of the spectral acceleration curves generated

by SSI analysis are presented in Fig 8. The results show mostly good agreements with those nodes in a frequency range from 0.1 Hz to 0.6 Hz. Considering the peak values at 4 Hz frequency, a range from 30 % to 100 % amplification can be observed for node no. 247, 248 and 249 corresponding to the node no. 246. It indicates that the higher elevation shows higher acceleration especially at the second or third peak.

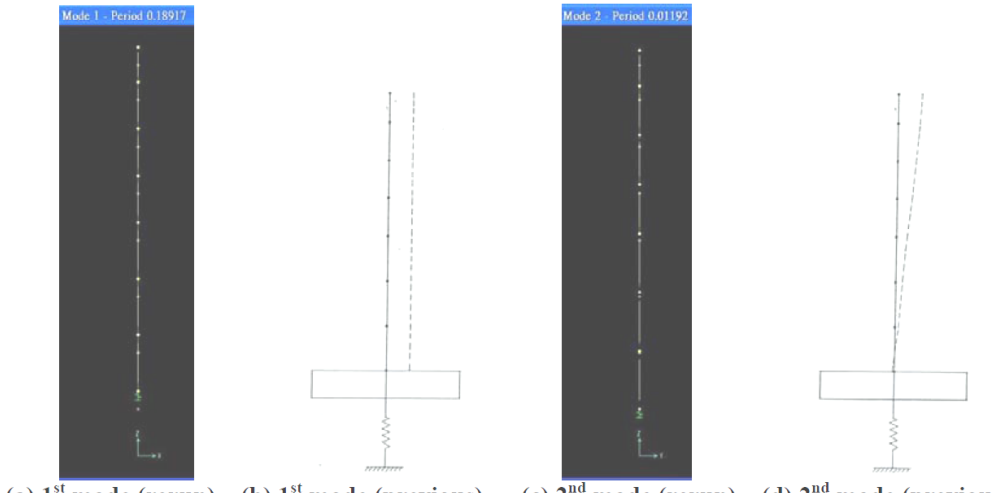

Fig. 6. Comparison of the natural frequency mode shape in the rerun and previous horizontal models

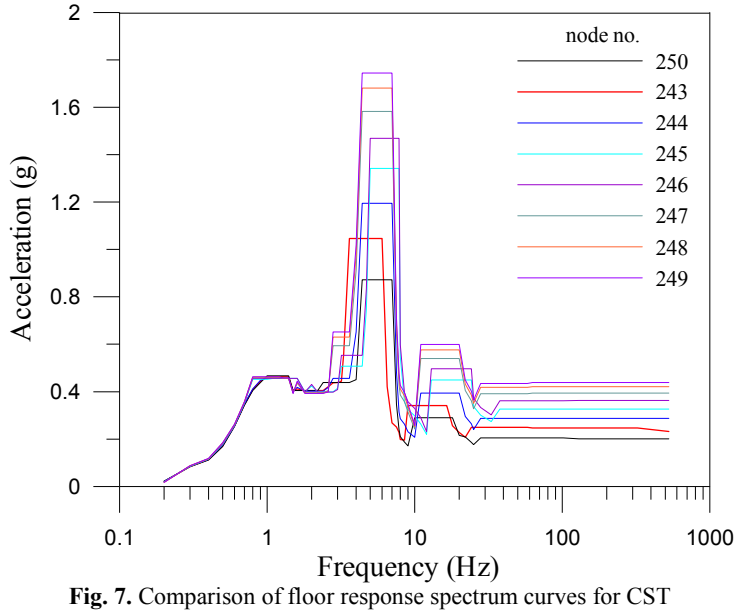

Fig. 7. Comparison of floor response spectrum curves for CST

Comparisons of the spectral acceleration curves for the spring model and SASSI model are illustrated in Fig. 9. From those results, there is no significant amplification below the frequency from 0.1 Hz to 1 Hz. The effect of magnification on the frequency range from 3 Hz to 7 Hz of spring model is more significant than on that of SASSI model. A significant difference is observed for the frequency range of 3 to 500 Hz and the node at higher elevation

demonstrates a greater magnification effect than the basemat. The ZPA and peak acceleration at the CST nodes are listed in Table 5. For those nodes, the SASSI model has lower ZPA and peak values than the spring model. In addition, the primary peak frequency of the SASSI model is significantly shorter than that of the spring model. Due to stiff soil and uncertainties concerning the properties of the soil and structure, there was a decreased SSI effect on the CST model.

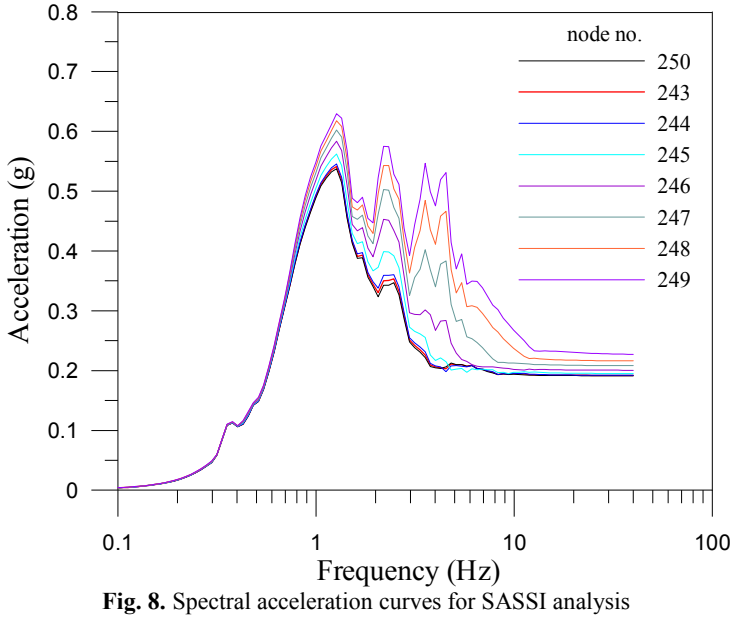

Fig. 8. Spectral acceleration curves for SASSI analysis

Table 5. The ZPA and peak values of CST model (unit: g)

Node	Description	ZPA for spring model	ZPA for SASSI model	Peak value for spring model	Peak value for SASSI model
250	Basemat	0.1874	0.1912	0.8722	0.5376
243		0.2288	0.1918	1.0462	0.5414
244		0.2646	0.1922	1.1942	0.5455
245		0.3017	0.1950	1.3420	0.5623
246		0.3335	0.2005	1.4689	0.5838
247		0.3622	0.2082	1.5825	0.6027
248		0.3870	0.2161	1.6808	0.6178
249	Top	0.4026	0.2272	1.7442	0.6298

Conclusions

The effect of SSI on dynamic behavior is an important issue that should be included in seismic analysis when structures are stiff and the soil is soft. In this study, the results of the natural frequency analysis and floor response spectrum curve reveal that the rebuilt spring model of CST conforms to the previous model generated in 1986. The natural frequency and mode shape provided by the proposed lumped mass stick model represent the overall building responses in a reasonable fashion. The SASSI model for SSI analysis is compared with the spring model. The spectral acceleration curves of SASSI model are significantly minified over the entire frequency range compared to the spring model. Comparison of the spring model, the spectral acceleration curves, ZPA, peak value significantly decrease due to the SSI effect. The

amplification effect becomes more obvious for the nodes at higher elevation. Variations in the SSI results were caused by stiff soil and uncertainties concerning the properties of the soil and structure. In the future, SSI models could also be used to establish the essential parameters required for soil structure interaction analyses including embedment depth, soil-basement separation, mesh size, and the properties of the structure and soil.

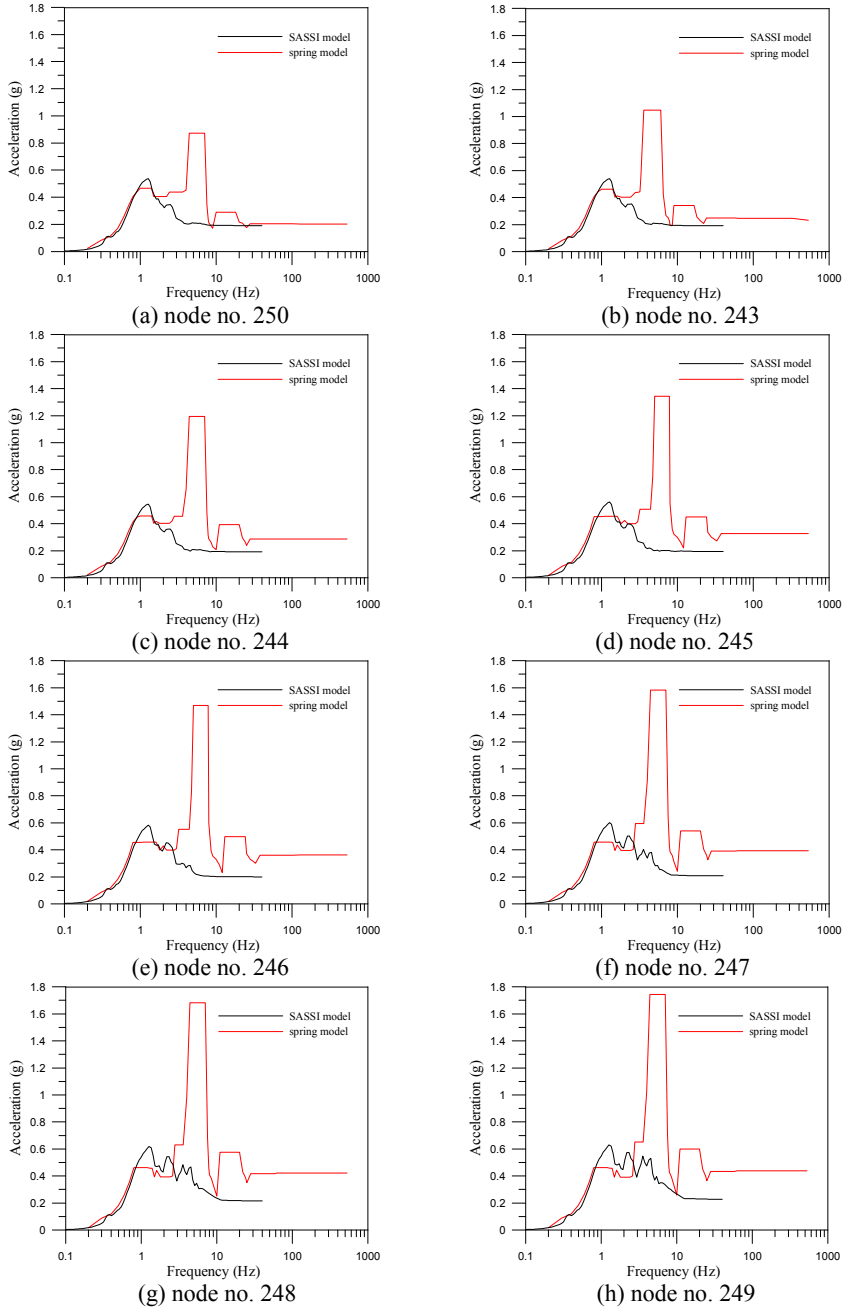

Fig. 9. Comparison of various nodes between spring model and SASSI model

References

[1] **Takahashi T. I., Goto M., Yoshida H., Sumino H., Matsui H.** Infectious diseases after the 2011 Great East Japan earthquake. Journal of Experimental & Clinical Medicine, Vol. 4, Issue 1, 2012, p. 20 – 23.

[2] **Kakinami Y., Masashi K., Liu J. Y., Watanabe S., Mogi T.** Ionospheric disturbance associated with radiation accidents of Fukushima I nuclear power plant damaged by the M9.0 2011 Tohoku earthquake. Advances in Space Research, Vol. 48, Issue 10, 2011, p. 1613 – 1616.

[3] **Lou M. L., Wang H. F., Chen X., Zhai Y. M.** Structure-soil-structure interaction: Literature review. Soil Dynamics and Earthquake Engineering, Vol. 31, Issue 12, 2011, p. 1724 – 1731.

[4] **Wolf J. P.** Dynamic Soil-Structure Interaction. Prentice-Hall, Inc., Englewood Cliffs, New Jersey, 1985.

[5] **Mylonakis G., Gazetas G., Nikolaou S., Michaelides O.** The role of soil on the collapse of 18 piers of the Hanshin expressway in the Kobe earthquake. Proceedings of 12th World Conference on Earthquake Engineering, January 1 - February 4, 2000, Auckland, New Zealand.

[6] USNRC Standard Review Plan. NUREG-0800: 3.7.2, Seismic System Analysis, Revision 3, 2007.

[7] **Saxena N., Paul D. K., Kumar R.** Effects of slip and separation on seismic SSI response of nuclear reactor building. Nuclear Engineering and Design, Vol. 241, Issue 1, 2011, p. 12 – 17.

[8] **Ghiocel D. M., Wilson P. R., Thomas G. G., Stevenson J. D.** Seismic response and fragility evaluation for an Eastern US NPP including soil-structure interaction effects. Reliability Engineering and System Safety, Vol. 62, Issue 3, 1998, p. 197 – 214.

[9] **Králik J., Šimonovič M.** Earthquake response analysis of nuclear power plant buildings with soil-structural interaction. Journal Mathematics and Computers in Simulation, Vol. 50, Issue 1-4, 1999, p. 227 – 236.

[10] **Kobayashi T., Yoshikawa K., Takaoka E., Nakazawa M., Shikama Y.** Time history nonlinear earthquake response analysis considering materials and geometrical nonlinearity. Nuclear Engineering and Design, Vol. 212, Issues 1-3, 2002, p. 145 – 154.

[11] **Tyapin A.** The frequency-dependent elements in the code SASSI: A bridge between civil engineers and the soil-structure interaction specialists. Nuclear Engineering and Design, Vol. 237, Issues 12-13, 2007, p. 1300 – 1306.

[12] **Zaicenco A., Alkaz V.** Soil-structure interaction effects on an instrumented building. Bulletin of Earthquake Engineering, Vol. 5, Issue 4, 2007, p. 533 – 547.

[13] Taiwan Power Company**.** Report of Seismic Analysis and Floor Response Spectrum Regeneration for Nuclear Power Station, 1986.

[14] **Yeh C. S., Lin T. W., Lai T. S.** EPRI/NRC/TPC SSI Workshop on Validation of Seismic Soil-Structure Interaction Analysis Techniques Using Lotung Experiment Data. December 9-11, 1987, Palo Alto, CA, USA.

